frontiers in Genetics

ORIGINAL RESEARCH
published: 11 January 2021
doi: 10.3389/fgene.2020.605378

Increased Expression of *TICRR* Predicts Poor Clinical Outcomes: A Potential Therapeutic Target for Papillary Renal Cell Carcinoma

Shuang Xia[1†], Yan Lin[2†], Jiaqiong Lin[3], Xiaoyong Li[4], Xuexian Tan[5] and Zena Huang[6]*

[1] Department of Cardiology, Guangdong Cardiovascular Institute, Guangdong Provincial Key Laboratory of Coronary Heart Disease Prevention, Guangdong Provincial People's Hospital, Guangdong Academy of Medical Sciences, Guangzhou, China, [2] Department of Nephrology, The Third Affiliated Hospital of Guangzhou Medical University, Guangzhou, China, [3] Department of Medical Genetics, School of Basic Medical Sciences, Southern Medical University, Guangzhou, China, [4] Department of Surgery, The Third Affiliated Hospital of Guangzhou Medical University, Guangzhou, China, [5] Department of Pathology, The Third Affiliated Hospital of Guangzhou Medical University, Guangzhou, China, [6] Department of General Medicine, Guangdong Provincial Geriatrics Institute, Guangdong Provincial People's Hospital, Guangdong Academy of Medical Sciences, Guangzhou, China

OPEN ACCESS

Edited by:
Yanni Sun,
City University of Hong Kong, Hong Kong

Reviewed by:
Xiangqian Guo,
Henan University, China
Ka-Chun Wong,
City University of Hong Kong, Hong Kong

***Correspondence:**
Zena Huang
506647168@qq.com

[†] These authors have contributed equally to this work

Specialty section:
This article was submitted to Computational Genomics, a section of the journal Frontiers in Genetics

Received: *12 September 2020*
Accepted: *07 December 2020*
Published: *11 January 2021*

Citation:
Xia S, Lin Y, Lin J, Li X, Tan X and Huang Z (2021) Increased Expression of TICRR Predicts Poor Clinical Outcomes: A Potential Therapeutic Target for Papillary Renal Cell Carcinoma. Front. Genet. 11:605378. doi: 10.3389/fgene.2020.605378

Background: Papillary renal cell carcinoma (PRCC), although the second-most common type of renal cell carcinoma, still lacks specific biomarkers for diagnosis, treatment, and prognosis. TopBP1-interacting checkpoint and replication regulator (*TICRR*) is a DNA replication initiation regulator upregulated in various cancers. We aimed to evaluate the role of *TICRR* in PRCC tumorigenesis and prognosis.

Methods: Based on the Kidney Renal Papillary cell carcinoma Project (KIRP) on The Cancer Genome Atlas (TCGA) database, we determined the expression of *TICRR* using the Wilcoxon rank sum test. The biological functions of *TICRR* were evaluated using the Metascape database and Gene Set Enrichment Analysis (GSEA). The association between *TICRR* and immune cell infiltration was investigated by single sample GSEA. Logistic analysis was applied to study the correlation between *TICRR* expression and clinicopathological characteristics. Finally, Cox regression analysis, Kaplan–Meier analysis, and nomograms were used to determine the predictive value of *TICRR* on clinical outcomes in PRCC patients.

Results: *TICRR* expression was significantly elevated in PRCC tumors ($P < 0.001$). Functional annotation indicated enrichment with negative regulation of cell division, cell cycle, and corresponding pathways in the high *TICRR* expression phenotype. High *TICRR* expression in PRCC was associated with female sex, younger age, and worse clinical stages. Cox regression analysis revealed that *TICRR* was a risk factor for overall survival [hazard ratio (HR): 2.80, $P = 0.002$], progression-free interval

(HR: 2.86, $P < 0.001$), and disease-specific survival (HR: 7.03, $P < 0.001$), especially in patients with male sex, age below 60 years, clinical stages II–IV and clinical T stage T1–T2.

Conclusion: Increased *TICRR* expression in PRCC might play a role in tumorigenesis by regulating the cell cycle and has prognostic value for clinical outcomes.

Keywords: *TICRR*, papillary renal cell carcinoma, clinical outcome, Treslin, immune infiltration

INTRODUCTION

Renal cell carcinoma (RCC) is a life-threatening cancer worldwide, ranking sixth among the most commonly diagnosed cancers in men and 10th in women (Siegel et al., 2018). Papillary RCC (PRCC) is the second most common type of RCC, accounting for nearly 18% of RCC (Srigley et al., 2013). In addition, it is the most common histological subtype in pediatric RCC and has been reported in 18% of dialysis patients (Morabito et al., 2010). However, diagnosis, treatment, and prognosis of PRCC are now mostly based on histological features, whose subtyping remains unsatisfactory (Fernandes and Lopes, 2015). Recent studies have introduced several novel biomarkers for RCC diagnosis and prognosis, such as urine aquaporin-1 and perilipin-2 (Farber et al., 2017; Cao et al., 2018; Song et al., 2019). However, these studies were mostly carried out in patients with rough RCC or clear cell RCC, lacking specific result for PRCC. An immunohistochemical marker α-methylacyl coenzyme A racemase was used for identifying PRCC (Alshenawy, 2015), while it was unrelated with PRCC prognosis. Several mutated genes were proved to be associated with PRCC diagnosis and treatment, including *MET*, *NF2*, *SETD2*, and Nrf2 pathway genes. Unfortunately, they were not sensitive enough, as they were only found in about 10 to 15% of PRCC (Akhtar et al., 2019). Therefore, it is urgent to search for a more convincing and suitable biomarker for PRCC.

TopBP1-interacting checkpoint and replication regulator (*TICRR*), also known as Treslin, is a critical DNA replication initiation regulator mediated by cyclin-dependent kinases and a DNA damage checkpoint (Boos et al., 2011). Biologically, *TICRR* regulates the cell cycle via determining S-phase progression from the expression level to epigenetic control (Charrasse et al., 2017; Maya-Mendoza et al., 2018) and thus promotes DNA replication. Overexpression of *TICRR* has been observed in several cancers, such as breast invasive carcinoma and liver hepatocellular carcinoma (Yu et al., 2019). It is associated with tumorigenesis, resistance to chemotherapy, and poor clinical outcomes (Yu et al., 2019). However, the potential role and underlying mechanism of *TICRR* in PRCC is not clear yet.

Using the RNA sequencing and clinical data of PRCC patients retrieved from The Cancer Genome Atlas (TCGA) database, we carried out a bioinformatics analysis to identify the significance of *TICRR* in PRCC tumorigenesis and prognosis. We observed an overexpression of *TICRR* in PRCC and investigated its potential role in PRCC tumorigenesis. Next, we performed a correlation analysis between *TICRR* and several clinicopathological characteristics. Finally, we identified the diagnostic and prognostic values of *TICRR*. This study provides novel insight into the underlying mechanisms of PRCC tumorigenesis and revealed *TICRR* as a potential diagnostic and prognostic biomarker in PRCC.

MATERIALS AND METHODS

Data Processing and Ethics Statement

We downloaded high-throughput sequencing RNA data [fragments per kilobase per million (FPKM) format] and corresponding clinicopathological information from the Kidney Renal Papillary cell carcinoma Project (KIRP) on the TCGA database[1]. Excluding three patients with incomplete clinicopathological information, a total of 288 PRCC patients were enrolled. RNA sequencing data were transformed from FPKM format to transcripts per million reads for this study. As the TCGA database is open to the public under specific guidelines, it confirms that all written informed consents were obtained before data collection.

Differentially Expressed Genes in Papillary Renal Cell Carcinoma Tumors

In total, 288 PRCC patients were separated into high- and low-*TICRR* expression groups according to *TICRR* median value. The R package "DESeq2"(Love et al., 2014) was used to identify differentially expressed genes (DEGs) between the two groups by a two-tailed hypothetical test based on the negative binomial generalized linear models, where the log-fold change larger than 1.5 and an adjusted *P*-value less than 0.05 were set as thresholds. The R packages "pheatmap" (Kolde, 2019) and "EnhancedVolcano" (Blighe, 2019) were applied to present results as heatmaps and volcano plots.

Functional Annotation of *TICRR*-Associated Differentially Expressed Genes in Papillary Renal Cell Carcinoma Tumors

The identified DEGs were then processed for functional annotation on the Metascape database[2] and online tool (Zhou et al., 2019). Minimum counts larger than 3, enrichment factors larger than 1.5, and a *P*-value less than 0.01 were set as analysis thresholds. Further, the R package "clusterProfiler" (Yu et al.,

[1]https://portal.gdc.cancer.gov/

[2]http://metascape.org

2012) was utilized for the Gene Set Enrichment Analysis (GSEA) (Subramanian et al., 2005) of the DEGs in the two groups. In GSEA, C2: curated gene sets from MSigDB collections were selected as reference gene sets. In total, 404 clusters were identified; clusters with a false discovery rate (FDR) less than 0.25 and *P*-value less than 0.05 were identified as significant. Protein–protein interaction (PPI) networks were investigated based on STRING database[3] (Szklarczyk et al., 2019) and visualized using Cytoscape software (v3.7.1) (Shannon et al., 2003).

Association of *TICRR* and Immune Cell Infiltration in Papillary Renal Cell Carcinoma Tumors

First, we used the single sample GSEA method from the R package "GSVA" (Hänzelmann et al., 2013) to present infiltration enrichment of 24 common immune cells, including dendritic cells (DCs), immature DCs (iDCs), activated DCs (aDCs), plasmacytoid DCs (pDCs), T cells, T helper (Th) cells, type 1 Th cells (Th1), type 2 Th cells (Th2), type 17 Th cells (Th17), regulatory T cells (Treg), T gamma delta (Tgd), T central memory (Tcm), T effector memory (Tem), T follicular helper (Tfh), CD8 + T cells, B cells, neutrophils, macrophages, cytotoxic cells, mast cells, eosinophils, natural killer (NK) cells, NK 56- cells, and NK 56 + cells. Next, the association between *TICRR* expression and immune cell infiltration was evaluated by Spearman's analysis, and the infiltration levels of immune cells were compared for high- and low-*TICRR* expression groups by Wilcoxon rank sum test.

Correlation Analyses for *TICRR* Expression and Clinicopathological Characteristics of Papillary Renal Cell Carcinoma Patients

Clinicopathological characteristics were compared for high- and low-*TICRR* expression groups using the Wilcoxon rank sum test (continuous variables) or Pearson's chi-square test

[3]http://string-db.org

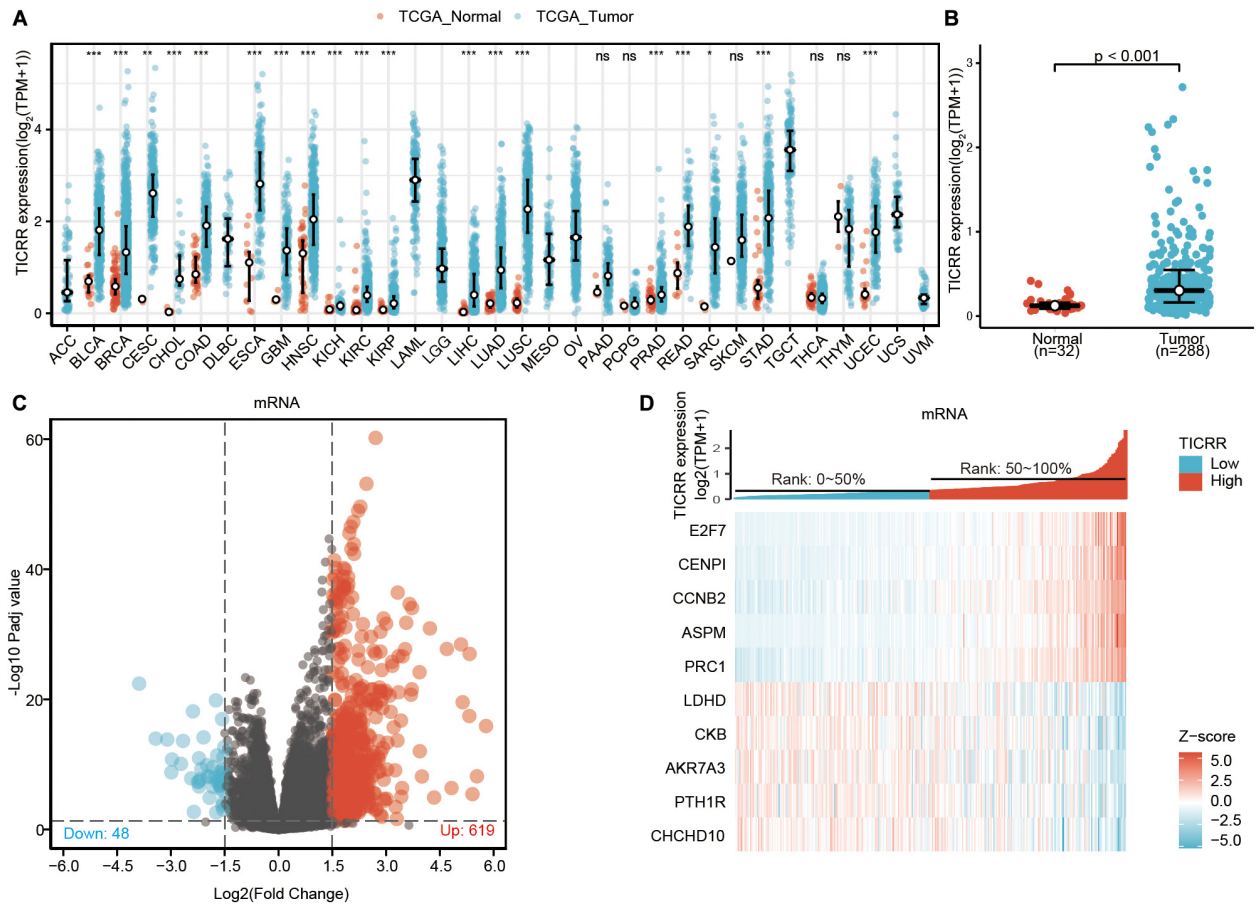

FIGURE 1 | Differential mRNA expression profiles in papillary renal cell carcinoma (PRCC) patients stratified by *TICRR* levels. **(A)** The comparison of *TICRR* expression between tumor and pericarcinous tissue in different types of cancers based on TCGA database. ns, $P \geq 0.05$; *$P < 0.05$; **$P < 0.01$; ***$P < 0.001$. **(B)** *TICRR* expression is higher in PRCC tumors than pericarcinous tissue. Based on the median *TICRR* level, 288 PRCC patients from The Cancer Genome Atlas –Kidney Renal Papillary cell carcinoma Project (TCGA-KIRP) were stratified into high- and low-*TICRR* expression groups. Shown are expression profiles of mRNA in two groups; and data are presented by volcano plots **(C)** and heatmaps **(D)**.

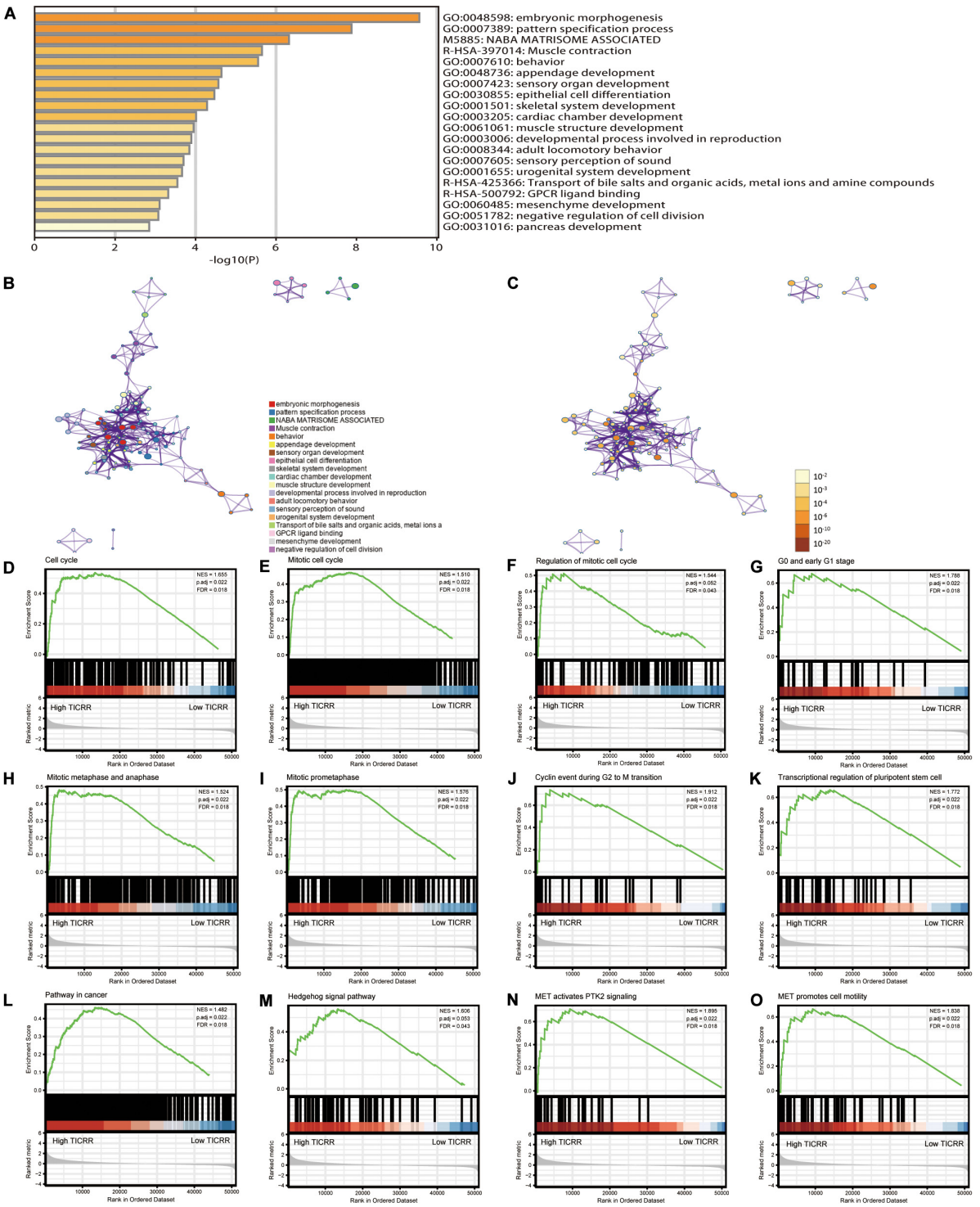

FIGURE 2 | Functional annotation of differentially expressed genes (DEGs) in papillary renal cell carcinoma (PRCC) patients with distinct *TICRR* levels. According to the Metascape database, 691 differentially expressed mRNAs between high- and low-*TICRR* expression groups were used for functional annotation. All statistically enriched terms were identified and then hierarchically clustered into a tree **(A)** based on the threshold of kappa score as 0.3. Representative terms from the cluster were converted into a network layout **(B)**. The size of a node is proportional to the number of input genes that fall into that term, and the respective color represents its cluster identity. Terms with a similarity score >0.3 are linked by an edge (the thickness of the edge represents the similarity score). The same enrichment network presents nodes colored by the *P*-value **(C)**. **(D–O)** Representative Gene Set Enrichment Analysis of differentially expressed mRNAs between high- and low-*TICRR* expression groups.

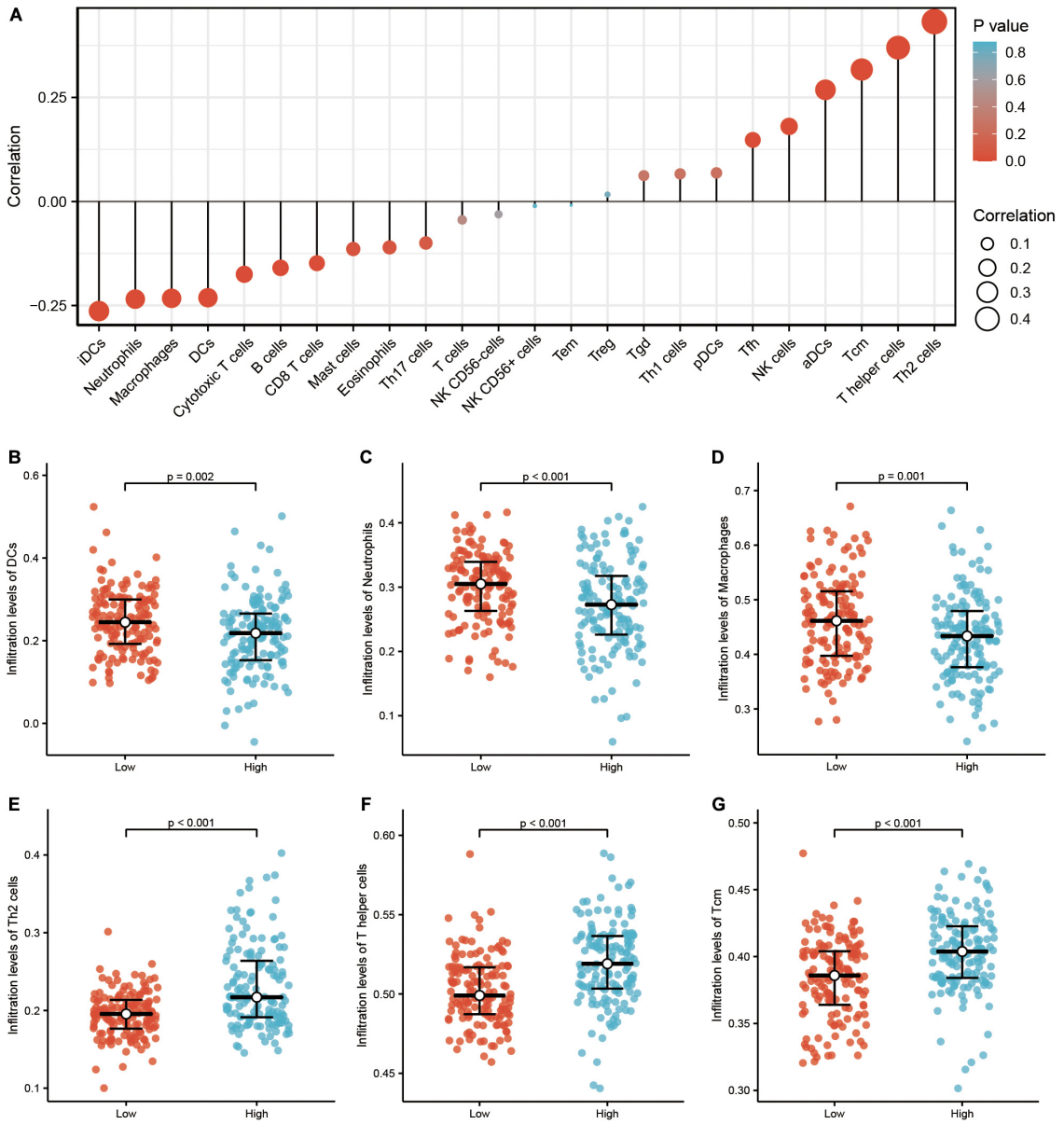

FIGURE 3 | Correlation of immune cell infiltration and *TICRR* expression in papillary renal cell carcinoma (PRCC) patients. **(A)** Relationships among infiltration levels of 24 immune cell types and *TICRR* expression profiles by Spearman's analysis. Shown is the comparison of infiltration levels of most correlated immune cells, including dendritic cells **(B)**, neutrophils **(C)**, macrophages **(D)**, type 2 T helper cells (Th2) cells **(E)**, Th cells **(F)**, and Tcm memory cells **(G)** between high- and low-*TICRR* expression groups. DCs, dendritic cells; aDCs, activated DCs; iDCs, immature DCs; pDCs, plasmacytoid DCs; Th, T helper cells; Th1, type 1 Th cells; Th2, type 2 Th cells; Th17, type 17 Th cells; Treg, regulatory T cells; Tgd, T gamma delta; Tcm, T central memory; Tem, T effector memory; Tfh, T follicular helper; NK, natural killer.

(rank variables). The correlation between *TICRR* expression and clinicopathological characteristics was evaluated by logistic analysis.

Clinical Significance of *TICRR* Expression in Papillary Renal Cell Carcinoma

TICRR expression was compared between PRCC tumors and pericarcinous tissues by receiver operating characteristic (ROC) analysis to test the predictive value of *TICRR* for PRCC diagnosis. Information on PRCC patients' clinical outcome was obtained from a published study (Liu et al., 2018), including overall survival, progression-free interval, and disease-specific survival. Kaplan–Meier (K-M) analysis, univariate, and multivariate Cox regression analysis were employed for prognosis analysis. The R package "randomForest" (Svetnik et al., 2003) was used for random forest regression. The R package "rms" (Harrell, 2020) was used to construct nomograms and calibration plots. The R package "forestplot" (Max Gordon, 2020) was applied for the

clinicopathological subgroup study. The above statistical analyses were all carried out by R (v4.0.0), with *P*-values less than 0.05 considered significant.

RESULTS

Expression Profiles of *TICRR* in Different Cancers and Related Differentially Expressed Genes in Papillary Renal Cell Carcinoma

Based on TCGA database, we determined the expression of *TICRR* mRNA in different cancers. As shown in **Figure 1A**, among 33 cancer types, the *TICRR* was significantly highly expressed in 19 cancers, especially in tumors located in gastrointestinal and urogenital tracts. More specifically, *TICRR* expression was much higher in PRCC tumors than in pericarcinous tissues ($P < 0.001$, **Figure 1B**). Interestingly, in none of the investigated cancer profiles was *TICRR* expression significantly decreased.

TABLE 1 | Clinicopathological characteristics of PRCC patients with differential *TICRR* expression.

Characteristic	Level	Low-*TICRR* group (*n* = 144)	High-*TICRR* group (*n* = 144)
Sex (%)*	Female	24 (16.7%)	52 (36.1%)
Age (median [IQR])*		64.00 [57.00, 71.00]	59.00 [51.00, 69.00]
Race (%)	Asian	1 (0.7%)	5 (3.6%)
	Black or African American	30 (22.4%)	30 (21.9%)
	White	103 (76.9%)	102 (74.5%)
Smoker (%)		65 (52.0%)	65 (53.7%)
Clinical T stage (%)*	T1	80 (77.7%)	59 (60.2%)
	T2	13 (12.6%)	13 (13.3%)
	T3	10 (9.7%)	25 (25.5%)
	T4	0 (0.0%)	1 (1.0%)
Clinical N stage (%)*	N0	72 (93.5%)	60 (78.9%)
	N1	5 (6.5%)	14 (18.4%)
	N2	0 (0.0%)	2 (2.6%)
Clinical M stage (%)	M0	101 (96.2%)	98 (95.1%)
	M1	4 (3.8%)	5 (4.9%)
Clinical stage (%)*	Stage I	80 (78.4%)	58 (60.4%)
	Stage II	12 (11.8%)	9 (9.4%)
	Stage III	7 (6.9%)	22 (22.9%)
	Stage IV	3 (2.9%)	7 (7.3%)
Serum calcium (%)	Normal	69 (75.0%)	64 (72.7%)
	Elevated	2 (2.2%)	4 (4.5%)
	Low	21 (22.8%)	20 (22.7%)
Hemoglobin (%)	Normal	64 (61.0%)	48 (46.6%)
	Elevated	0 (0.0%)	1 (1.0%)
	Low	41 (39.0%)	54 (52.4%)
MET status (%)	Mut	6 (4.3%)	14 (10.1%)

*IQR, interquartile range; PRCC, papillary renal cell carcinoma. *p < 0.05.*

Based on the median *TICRR* expression in PRCC tumors, 288 PRCC patients were stratified into two groups, high- and low-*TICRR* expression groups. We next compared mRNA, miRNA, and lncRNA expression between the two groups. Finally, 667 mRNAs (619 upregulated and 48 downregulated, **Figure 1C**), 2 miRNAs (2 upregulated, **Supplementary Figure 1**), and 341 lncRNAs (316 upregulated and 25 downregulated, **Supplementary Figure 1**) were recognized as DEGs (absolute value of fold change >1.5, $P < 0.05$) in the high-*TICRR* group. Representative DEGs were also illustrated by heatmaps (**Figure 1D** and **Supplementary Figure 1**).

Functional Annotation of *TICRR*-Associated Differentially Expressed Genes in Papillary Renal Cell Carcinoma Tumors

In order to evaluate the function of *TICRR*-associated DEGs in PRCC patients, the software "Metascape" was applied. As presented in **Figures 2A–C** and **Supplementary Table 1**, we found that several PRCC-related pathways were enriched, including epithelial cell differentiation (GO: 0030855, $P < 0.001$, enrichment factor = 2.654, FDR = 0.037), urogenital system development (GO: 0001655, $P < 0.001$, enrichment factor = 3.448, FDR = 0.141), and negative regulation of cell division (GO: 0051782, $P = 0.001$, enrichment factor = 15.802, FDR = 0.266). Moreover, the GSEA showed *TICRR*-associated DEGs significantly enriched in cell proliferation related clusters (**Figures 2D–K**), such as mitotic cell cycle [normalized enrichment score (NES) = 1.510, adjusted $P = 0.022$, FDR = 0.018], cyclin events during G2 to M transition (NES = 1.912, adjusted $P = 0.022$, FDR = 0.018), mitotic metaphase and anaphase (NES = 1.524, adjusted $P = 0.022$, FDR = 0.018), and mitotic prometaphase (NES = 1.576, adjusted $P = 0.022$, FDR = 0.018). *TICRR*-associated DEGs were also enriched in cancer pathways (**Figure 2L**), especially the cell cycle-related Hedgehog signaling pathway (**Figure 2M**). More interestingly, *TICRR*-associated DEGs were associated with the activity of the MET gene (**Figures 2N,O**), which is usually involved in oncogenesis. We also constructed a PPI network for DEGs (**Supplementary Figure 2**), where the *TICRR* served as the hub gene related to another eight genes.

Association of *TICRR* and Immune Cell Infiltration in Papillary Renal Cell Carcinoma Tumors

Infiltration of 24 immune cell types in PRCC was determined using the ssGSEA method first, and subsequently the association between *TICRR* and immune cell infiltration was investigated by Spearman's analysis. As shown in **Figure 3A**, Tcm ($R = 0.317$, $P < 0.001$), Th cells ($R = 0.317$, $P < 0.001$), and NK cells ($R = 0.180$, $P = 0.002$) were all positively correlated with *TICRR* expression. However, DCs ($R = -0.231$, $P < 0.001$), macrophages ($R = -0.233$, $P < 0.001$), neutrophils ($R = -0.235$, $P < 0.001$), and B cells ($R = -0.160$, $P = 0.007$) showed a negative association with *TICRR*. More specifically, we evaluated the infiltration levels of six most relevant immune cells—DCs (**Figure 3B**),

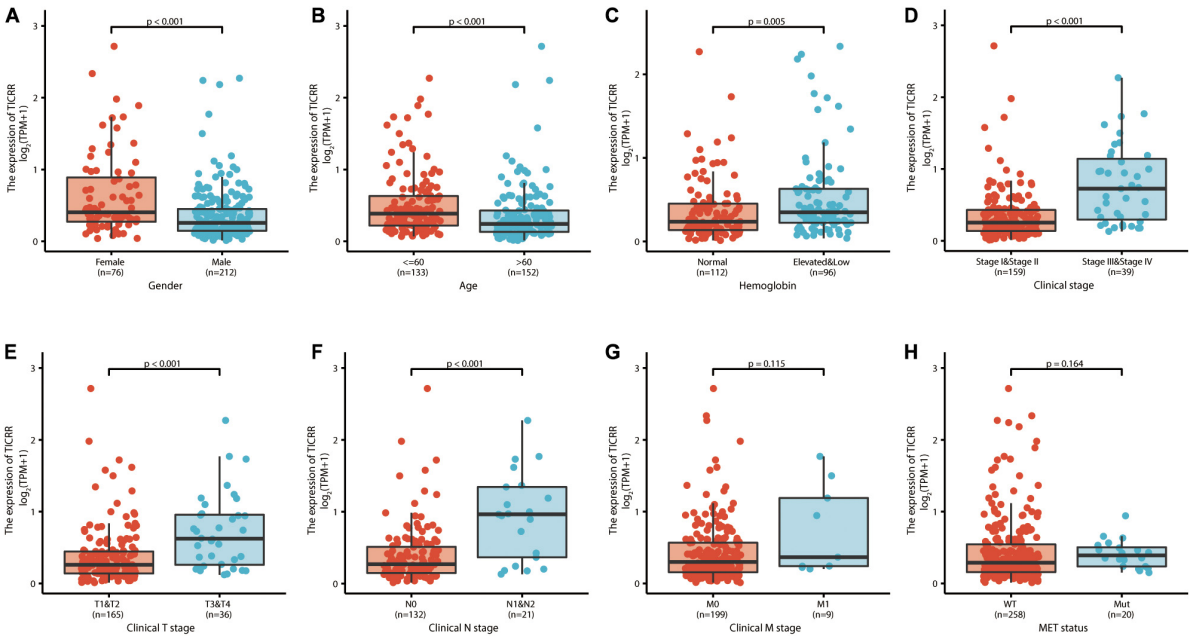

FIGURE 4 | *TICRR* expression is associated with clinicopathological characteristics in papillary renal cell carcinoma (PRCC) patients. The Wilcoxon rank sum test was applied to analyze the association of *TICRR* expression with sex **(A)**, age **(B)**, hemoglobin level **(C)**, clinical stage **(D)**, clinical T stage **(E)**, clinical N stage **(F)**, clinical M stage **(G)**, and MET status **(H)**.

TABLE 2 | Logistic regression analysis of association between clinicopathological characteristics and *TICRR* expression in PRCC patients.

Characteristic	Odds ratio (OR)	*P*-value
Clinical T stage (T3–T4 vs. T1–T2)	2.13 (1.29–3.79)	0.006
Clinical N stage (N1–N2 vs. N0)	2.64 (1.51–5.11)	0.002
Clinical M stage (M1 vs. M0)	1.60 (0.77–2.78)	0.115
Clinical stage (stage II–IV vs. stage I)	2.87 (1.61–5.72)	0.001
Serum calcium (abnormal vs. normal)	0.93 (0.48–1.59)	0.808
Hemoglobin (abnormal vs. normal)	1.74 (1.09–3.08)	0.032
MET status (Mut vs. WT)	0.71 (0.19–1.47)	0.501
Sex (Female vs. male)	2.22 (1.47–3.62)	<0.001
Age (>60 vs. ≤60)	0.66 (0.41–0.98)	0.054

PRCC, papillary renal cell carcinoma; WT, wild type; Mut, mutation.

neutrophils (**Figure 3C**), macrophages (**Figure 3D**), Th2 cells (**Figure 3E**), Th cells (**Figure 3F**), and Tcm (**Figure 3G**)—in distinct *TICRR* groups, which showed results consistent with those in **Figure 3A**.

Association of *TICRR* Expression and Clinicopathological Characteristics in Papillary Renal Cell Carcinoma Patients

We investigated the clinicopathological characteristics of PRCC patients with differential *TICRR* expression, as shown in **Table 1**. Compared with the low-*TICRR* group, patients in the high-*TICRR* group manifested a higher proportion of female sex, younger age, worse clinical stages, and more severe T and M stages. However, there was no significant difference in the distribution of clinical T stages, serum calcium concentration, hemoglobin level, or MET gene mutational status between two groups.

Further, we analyzed *TICRR* expression in patients with different clinicopathological characteristics. *TICRR* expression was significantly elevated in patients of female sex (**Figure 4A**), age below 60 years (**Figure 4B**), abnormal hemoglobin level (**Figure 4C**), clinical stages III and IV (**Figure 4D**), T stages T3 and T4 (**Figure 4E**), and N stages N1 and N2 (**Figure 4F**). As shown in **Table 1**, patients with different M stages (**Figure 4G**) and MET mutational status (**Figure 4H**) both shared similar *TICRR* expression levels. We also utilized logistics analysis to determine the correlation between *TICRR* expression and clinicopathological characteristics (**Table 2**). We found prominently positive correlations of *TICRR* expression with clinical stage (including T and N stages), hemoglobin, and female sex.

Predictive Value of *TICRR* for Papillary Renal Cell Carcinoma Diagnosis and Prognosis

In order to explore the clinical benefits of *TICRR* evaluation, we used a ROC curve to demonstrate its value on discriminating PRCC diagnosis. As the area under the curve (AUC) was 0.807, *TICRR* showed significant high sensitivity and specificity for PRCC diagnosis (**Figure 5A**). Next, K-M analyses were applied to verify the prediction of *TICRR* on clinical outcomes. As shown in **Figures 5B–D**, overall survival [hazard ratio (HR): 2.80, $P = 0.002$), progression-free interval (HR: 2.86, $P < 0.001$),

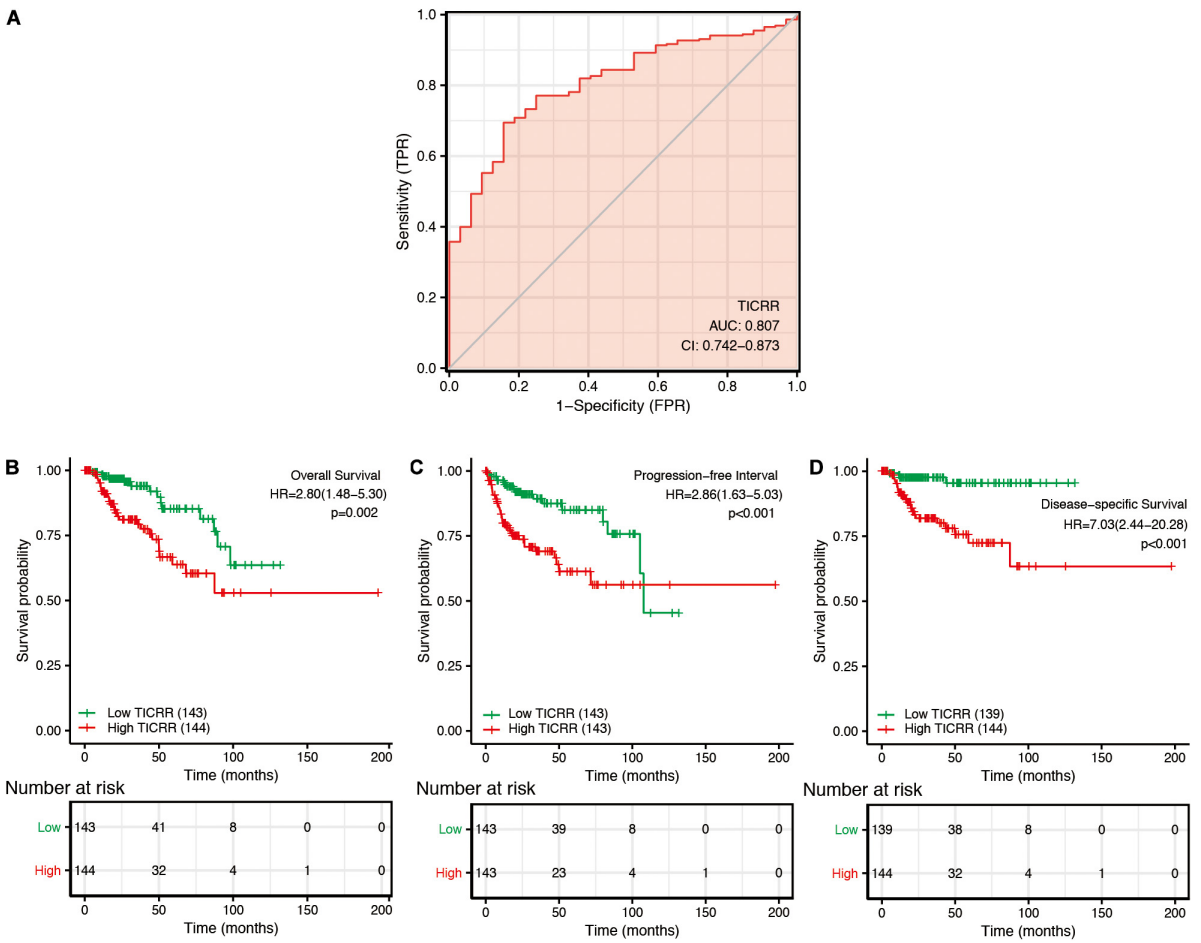

FIGURE 5 | Predictive value of *TICRR* expression for diagnosis and clinical outcomes in papillary renal cell carcinoma (PRCC) patients. **(A)** Receiver operating characteristic (ROC) curve analysis evaluating the performance of *TICRR* for PRCC diagnosis. Shown are the Kaplan–Meier analyses comparing overall survival **(B)**, progression-free interval **(C)**, and disease-specific survival **(D)** between high- and low-*TICRR* expression groups.

TABLE 3 | Cox regression analysis for clinical outcomes in PRCC patients.

Characteristics	HR for overall survival (95% CI)		HR for progression-free interval (95% CI)		HR for disease-specific survival (95% CI)	
	Univariate	Multivariate	Univariate	Multivariate	Univariate	Multivariate
Clinical T stage (T3–T4 vs. T1–T2)	4.687***	0.546	7.383***	1.923	8.926***	0.513
Clinical N stage (N1–N2 vs. N0)	10.637***	8.683*	17.022***	6.790 ∗∗	19.162***	7.111*
Clinical M stage (M1 vs. M0)	38.111***	16.622 ∗∗	10.324***	1.089	40.575***	20.996**
Clinical stage (stage II–IV vs. stage I)	5.123***	3.686	6.983***	1.976	27.918***	12.037*
Smoker (yes vs. no)	0.564		1.230		0.610	
Age (>60 vs. ≤60 years)	0.956		0.820		0.447*	1.321
Sex (male vs. female)	0.617		0.528		0.544	
Serum calcium (abnormal vs. normal)	1.659		1.180		1.749	
Hemoglobin (abnormal vs. normal)	4.381***	2.141	1.976*	2.137	3.174*	2.172
MET status (Mut vs. WT)	1.025		1.158		0.508	
Race (White vs. Black or African American and Asian)	0.921		0.863		0.891	
TICRR (high vs. low)	2.801**	3.862∗	2.859***	2.496	7.029***	4.705*

*HR, hazard ratio; PRCC, papillary renal cell carcinoma; WT, wild type; Mut, mutation; CI, confidence interval. *P < 0.05; **P < 0.01; ***P < 0.001.*

and disease-specific survival (HR: 7.03, $P < 0.001$) for high-*TICRR* groups were all statistically worse than those for the low-*TICRR* group.

Moreover, we performed a multivariate Cox regression analysis to further evaluate the predictive value of *TICRR* on clinical outcomes. As shown in **Table 3**, *TICRR* expression was an independent risk factor for overall survival (HR: 3.862, $P = 0.036$) and disease-specific survival (HR: 4.705, $P = 0.039$) in multivariate Cox regression, although it did not provide any significant predictive ability for progression-free interval. Conversely, clinical stage, especially clinical N and M stages, also showed predictive advantages for clinical outcomes in multivariate Cox regression analyses. In order to evaluate the importance of each predictive factor for clinical outcomes, we carried out a random forest analysis to predict overall survival. The random forest model reached an overall percentage accuracy of 86.8%. As shown in **Supplementary Figure 3**, *TICRR* expression ranked second among the most important predictors of overall survival in PRCC patients.

All the statistically significant prognostic factors in each multivariate Cox regression analysis were then used to construct a prognostic nomogram, and a calibration curve was drawn to test the efficiency of the nomogram. Clinical N and M stages, as well as *TICRR*, were included in the nomogram to predict

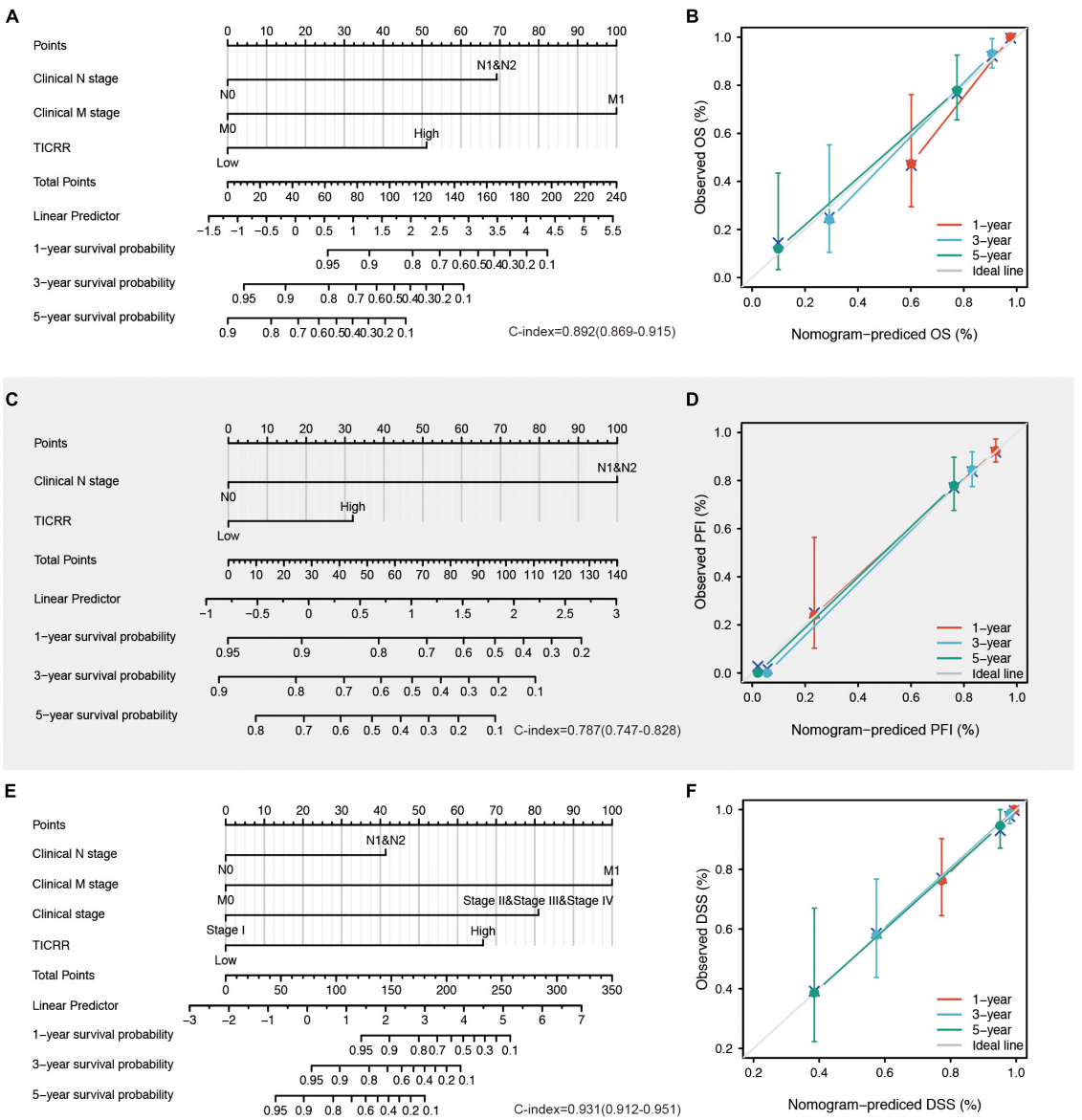

FIGURE 6 | Construction and validation of nomograms based on *TICRR* expression. Shown are the nomograms constructed to establish *TICRR* expression-based risk scoring models for 1-, 3-, and 5-year overall survival **(A)**, progression-free interval **(C)**, and disease-specific survival **(E)**. Calibration plots validating the efficiency of nomograms for overall survival **(B)**, progression-free interval **(D)**, and disease-specific survival **(F)**. OS, overall survival; PFI, progression-free interval; DSS, disease-specific survival.

overall survival, which had a C-index of 0.892 (**Figure 6A**). Clinical N and *TICRR* were included in a nomogram constructed to predict progression-free interval, which had a C-index of 0.787 (**Figure 6C**). Clinical stage, clinical N and M stages, and *TICRR* were used to construct a predictive nomogram for disease-specific survival, which had a C-index of 0.931 (**Figure 6E**). The calibration curves all presented desirable prediction of the three nomograms for the 1-, 3-, and 5-year clinical outcomes, with the exception of the 1-year prediction for overall survival, which was slightly underestimated (**Figures 6B,D,F**).

Prognostic Performance of *TICRR* in the Papillary Renal Cell Carcinoma Clinicopathological Subgroups

Next, we attempted to determine the predictive value of *TICRR* for clinical outcomes in several clinicopathological subgroups. We carried out Cox regression analyses in specific subgroups (**Table 4**). The results were also presented as forest plots (**Figure 7**). As shown in the forest plot in **Figure 7A**, *TICRR* was a significant risk factor for overall survival in patients of male sex (HR = 2.386, $P = 0.019$), age below 60 years (HR = 12.615, $P = 0.014$), clinical stage II–IV (HR = 3.740, $P = 0.019$), clinical T stages T1 and T2 (HR = 4.038, $P = 0.009$), clinical N0 stage (HR = 3.030, $P = 0.048$), clinical M0 stage (HR = 3.795, $P = 0.002$), and wild-type MET gene status (HR = 2.892, $P = 0.002$). Similar observations occurred for progression-free interval (**Figure 7B**) and disease-specific survival (**Figure 7C**). As there were few patients with clinical M1 stage (9 patients, occupying 4% of the sample) and MET mutation (20 patients, 7% of the sample), the subgroup analyses for clinical M1 stage and MET mutational status could not be performed. We also presented K-M analyses for clinical outcomes (overall survival, progression-free interval, and disease-specific survival) in the following four representative subgroups: male sex, age below 60 years, clinical stages II–IV, and T stages T1 and T2 (**Figure 8**). All the results demonstrated significantly better clinical outcomes in the low-*TICRR* expression groups.

DISCUSSION

In the present study, we focused on expression profiles, clinicopathological associations, and the clinical significance of a DNA replication initiation regulator, *TICRR*, in PRCC by analyzing datasets from the TCGA-KIRP. We observed prominent increased *TICRR* expression in PRCC tumors. DEGs related to higher *TICRR* levels were specifically enriched in cell cycle- and MET-associated pathways. We also revealed a marked association of *TICRR* expression with sex, age, and clinical stages in PRCC patients. Finally, we determined the predictive value of *TICRR* for overall survival, progression-free interval, and disease-specific survival in PRCC patients, especially in those of male sex, age below 60 years, and clinical stages II–IV and T stages T1–T2.

TABLE 4 | Prognostic performance of *TICRR* on clinical outcomes in PRCC patient subgroups by Cox regression analysis.

Characteristics	*N* (%)	HR for overall survival (95% CI)	HR for progression-free interval (95% CI)	HR for disease-specific survival (95% CI)
Sex				
Female	76 (26)	3.653 (0.805–16.585)	5.541 (1.275–24.081)*	N.A.
Male	211 (74)	2.386 (1.157–4.922)*	2.131 (1.110–4.090)*	4.831 (1.590–14.681)**
Age				
≤60	133 (47)	12.615 (1.682–94.637)*	2.732 (1.102–6.778)*	12.081 (1.606–90.905)*
>60	152 (53)	2.212 (0.983–4.980)	3.182 (1.469–6.892)**	3.846 (0.993–14.899)
Clinical stage				
Stage I	138 (70)	2.406 (0.675–8.577)	1.932 (0.648–5.759)	N.A.
Stage II–IV	60 (30)	3.740 (1.245–11.236)*	2.449 (1.012–5.927)*	3.740 (1.245–11.236)*
Clinical T stage				
T1–T2	165 (82)	4.038 (1.414–11.527)**	2.938 (1.226–7.037)*	12.189 (1.522–97.619)*
T3–T4	36 (18)	2.322 (0.637–8.461)	1.594 (0.556–4.575)	2.322 (0.637–8.461)
Clinical N stage				
N0	132 (86)	3.030 (1.012–9.076)*	2.531 (0.979–6.545)	9.620 (1.156–80.079)*
N1–N2	21 (14)	2.065 (0.570–7.477)	2.069 (0.632–6.775)	2.065 (0.570–7.477)
Clinical M stage				
M0	199 (96)	3.795 (1.602–8.992)**	2.979 (1.481–5.991)**	10.397 (2.389–45.253)**
M1	9 (4)	N.A.	N.A.	N.A.
MET status				
WT	257 (93)	2.892 (1.473–5.676)**	2.999 (1.638–5.488)***	6.904 (2.367–20.137)***
Mut	20 (7)	0.354 (0.022–5.659)	N.A.	N.A.
Hemoglobin				
Normal	112 (54)	4.097 (0.794–21.126)	2.346 (0.870–6.327)	8.275 (0.966–70.858)
Abnormal	96 (46)	1.587 (0.677–3.715)	1.887 (0.768–4.636)	2.470 (0.679–8.986)

*HR, hazard ratio; CI, confidence interval; WT, wild type; Mut, mutation. *P < 0.05; **P < 0.01; ***P < 0.001.*

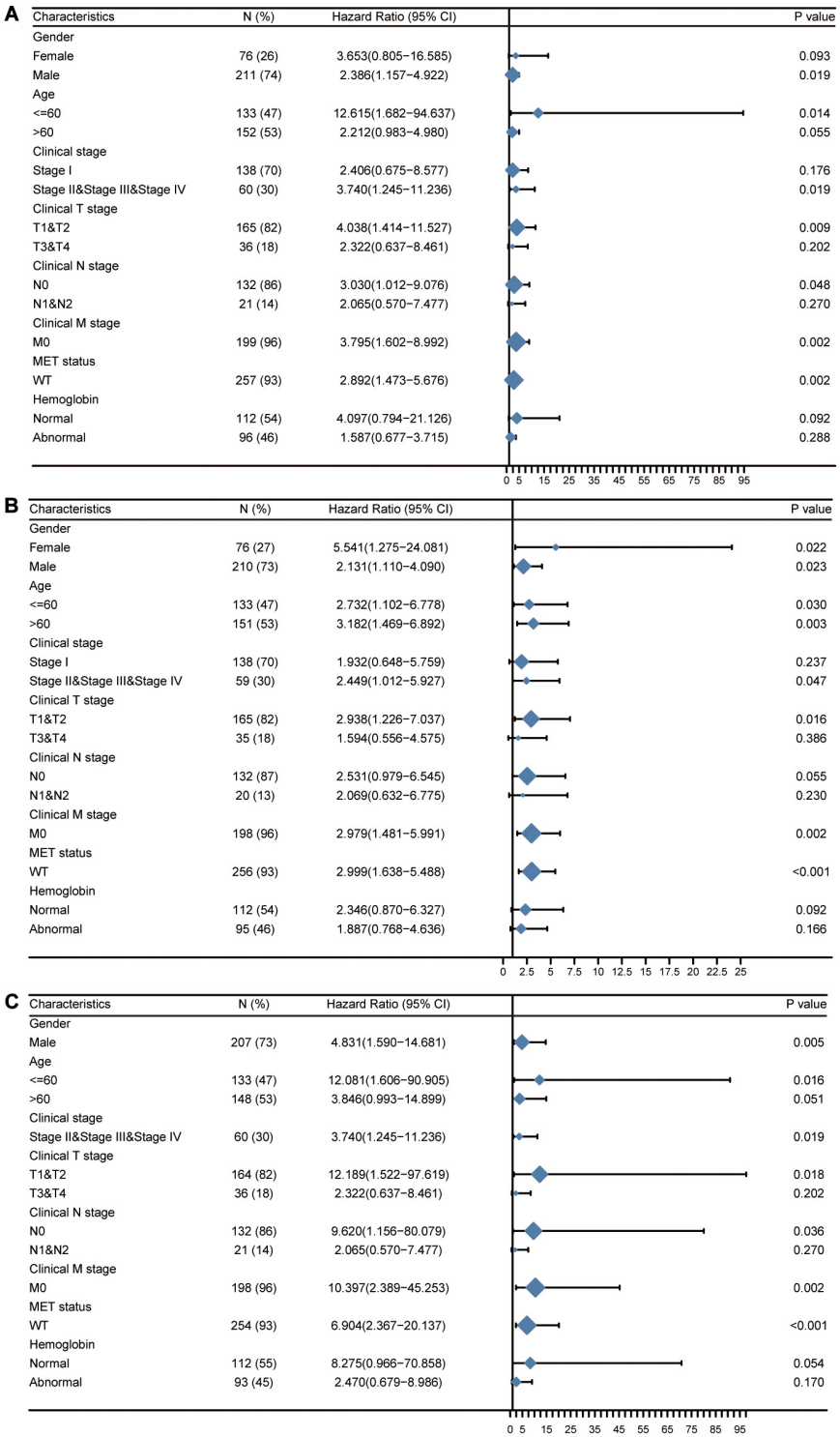

FIGURE 7 | Prognostic performance of *TICRR* on clinical outcomes in different papillary renal cell carcinoma (PRCC) patient subgroups. Patients were divided into different subgroups according to sex, age, clinical stage, clinical TNM stage, MET status, and hemoglobin level. For each subgroup, the prognostic performance of *TICRR* on overall survival **(A)**, progression-free interval **(B)**, and disease-specific survival **(C)** were evaluated by Cox regression, and the results are presented as hazard ratio. The bar represents the 95% confidence interval of hazard ratio, the diamond's size represents the significance of *TICRR*'s performance.

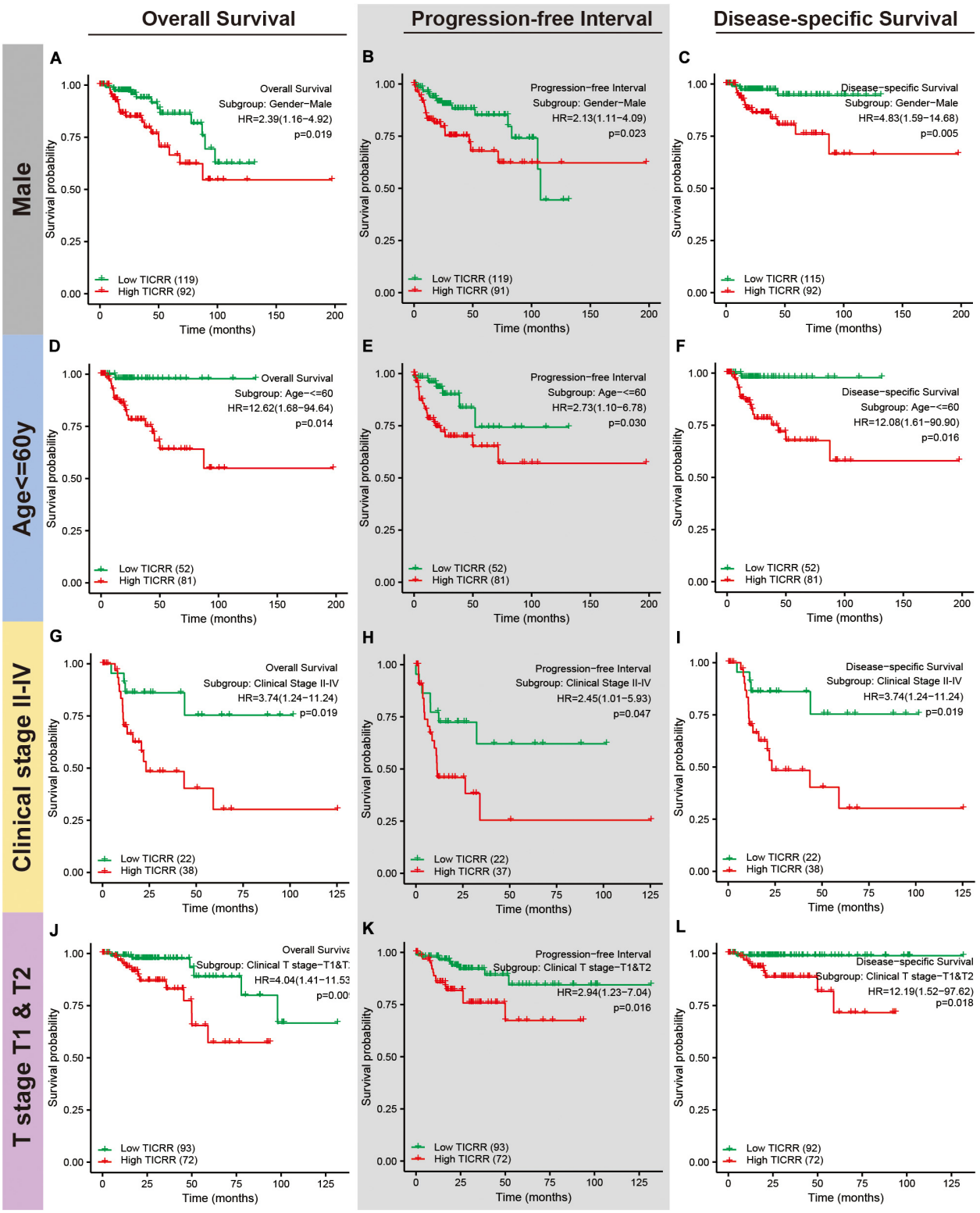

FIGURE 8 | Distinct clinical outcomes based on *TICRR* expression in papillary renal cell carcinoma (PRCC) patient subgroups. Kaplan–Meier analysis showing the comparison of overall survival **(A,D,G,J)**, progression-free interval **(B,E,H,K)**, and disease-specific survival **(C,F,I,L)** between high- and low-*TICRR* expression groups in several PRCC patient subgroups, including male sex **(A–C)**, age below 60 years **(D–F)**, clinical stage II–IV **(G–I)**, and T stages T1–T2 **(J–L)**.

Uncontrollable DNA replication and thus cell proliferation are an essential mechanism in tumorigenesis. As a critical DNA replication regulator, *TICRR* plays an important role in several solid cancers (Yu et al., 2019). In our study, we found that *TICRR* was significantly elevated in several urogenital cancers, including PRCC, chromophobe renal carcinoma, renal clear cell carcinoma, bladder urothelial carcinoma, cervical squamous cell carcinoma, and in endocervical adenocarcinoma. Moreover, *TICRR* was also upregulated in tumors of other organs, such as breast invasive carcinoma, colon adenocarcinoma, and glioblastoma multiforme. Thus, *TICRR* may be a crucial hub gene in tumorigenesis.

Further, we attempted to describe the potential functions and mechanisms involving *TICRR* in PRCC. Based on results from previous studies (Bruck and Kaplan, 2015; Bruck et al., 2015), *TICRR* coordinates the assembly and activation of the eukaryotic replication fork helicase, which further unwinds double-stranded DNA and initiates DNA replication. In our study, based on functional annotation of *TICRR*-associated DEGs, epithelial cell differentiation and urogenital system development were closely associated with *TICRR* expression. Moreover, *TICRR* was associated with negative regulation of cell division. Based on additional GSEA, several cell cycle-related events were enriched in the high-*TICRR* group. The above data all provided evidence that *TICRR* functions as a critical DNA replication initiation regulator in PRCC. In a different study focusing on breast cancer, *TICRR* showed a similar effect on tumorigenesis, as silencing of *TICRR* significantly inhibited DNA replication, arrested cell cycle progression, and activated DNA damage (Yu et al., 2019). More interestingly, we found that patients in the high-*TICRR* group more frequently harbored MET mutations, which represents an appealing drug target given its prevalence in PRCC. The functional annotation analysis revealed that higher *TICRR* levels were associated with increased pathophysiological activity of the MET gene. Therefore, *TICRR* expression might be of great importance in PRCC tumorigenesis by affecting MET status and function.

We also revealed an underlying relationship between *TICRR* expression and immune cell infiltration. *TICRR* expression was negatively correlated with DCs, macrophages, and neutrophils. As the most effective antigen presenting cells, DCs activate CD 8 + T cells by cross-priming and further initiate anti-tumor immunity (Fu and Jiang, 2018). In the following immune response, neutrophils and macrophages work together against tumors (Qu et al., 2018). Moreover, neutrophils proved to be associated with better prognosis in different cancers (Donskov, 2013). Therefore, overexpressed *TICRR* seemed to dampen tumor immunity, help cancer cells escape from elimination, and finally accelerate tumorigenesis. On the other hand, we found a significantly positive correlation between *TICRR* expression and Tcm infiltration. Tumor-infiltrated Tcm cells have been reported in multiple cancers (Beckhove et al., 2004), which often exhibit dysfunctional phenotypes correlating with cancer progression (Reading et al., 2018). It can be explained that excessive neoantigen exposure caused functionally altered Tcm cells that skewed the anti-tumor response toward non-responsiveness (Merad et al., 2013).

Another issue of interest was the clinical significance of *TICRR* in PRCC. The ROC curve for *TICRR* discrimination of PRCC diagnosis had an AUC of 0.807, strongly suggesting that *TICRR* was a convincing biomarker for PRCC diagnosis. Moreover, we demonstrated that higher *TICRR* expression was correlated with several clinicopathological characteristics: female sex, younger age, abnormal hemoglobin, and worse clinical stages. As most of the above characteristics were risk factors for survival in PRCC patients (Fernandes and Lopes, 2015; Peng et al., 2018), we proposed TICRR as a marker for poor survival in PRCC. According to further Cox regression analyses and nomograms, *TICRR* presented satisfactory performance on clinical outcomes in PRCC. Patients with higher *TICRR* levels showed strikingly worse overall survival, progression-free interval, and disease-specific survival. This prognostic value of *TICRR* seemed to be more prominent in patients with specific features: male sex, age below 60 years, and clinical stages II–IV and T stages T1–T2. Using an online tool LOGpc (Long-term Outcome and Gene Expression Profiling Database of pan-cancers)[4], *TICRR* was proved to be associated with lower overall survival in other tumors, such as renal clear cell carcinoma (Xie et al., 2019a), adrenocortical carcinoma (Xie et al., 2019b), breast invasive carcinoma (Yan et al., 2019), and lung cancer (Yan et al., 2020). The universal upregulation and predictive performance of *TICRR* indicated a possibility that it could represent a common prognostic biomarker for these cancer types.

Although we uncovered a potential mechanism for *TICRR* activity in PRCC tumorigenesis and its predictive value in PRCC clinical outcomes, our study still presented several limitations. First, because of the incomplete information about treatments and corresponding responses, we could not evaluate a specific role for *TICRR* in PRCC treatment. Second, we mainly focused on the RNA sequencing data from the TCGA database; thus, we were unable to provide information on relative protein levels or downstream pathways involving *TICRR*. Thus, these will remain areas for further *in vivo* and *in vitro* studies concentrating on the direct mechanism of *TICRR* activity in PRCC.

CONCLUSION

Increased *TICRR* expression in PRCC might play a role in tumorigenesis by regulating cell cycle and exhibiting prognostic value for clinical outcomes. This study sheds light on *TICRR* as a potential therapeutic target for PRCC.

DATA AVAILABILITY STATEMENT

Publicly available datasets were analyzed in this study. This data can be found here: https://portal.gdc.cancer.gov/.

ETHICS STATEMENT

All the data were collected and downloaded from TCGA database. As TCGA database is open to the public under specific

[4]http://bioinfo.henu.edu.cn/DatabaseList.jsp

guidelines, it is confirmed that all written informed consents were achieved. The patients/participants provided their written informed consent to participate in this study.

AUTHOR CONTRIBUTIONS

SX and YL: project investigation. XT: methodology. JL: writing–original draft. XL: writing–review and editing. ZH: project administration and supervision. All authors contributed to the article and approved the submitted version.

FUNDING

This study was supported by the Natural Science Foundation of Guangdong Province (No. 2018A030310016), Guangdong Provincial Medical Science Foundation (No. A2018110), and the Lab Opening-up Project for college students of Guangzhou Medical University.

SUPPLEMENTARY MATERIAL

The Supplementary Material for this article can be found online at: https://www.frontiersin.org/articles/10.3389/fgene.2020.605378/full#supplementary-material

Supplementary Figure 1 | Differential non-coding RNA expression profiles in PRCC patients stratified by *TICRR* levels. Expression profiles of miRNAs **(A,C)** and lncRNAs **(B,D)** in two groups are presented by volcano plots **(A,B)** and heatmaps **(C,D)**.

Supplementary Figure 2 | Protein-protein interaction networks of DEGs in PRCC patients with high- and low-*TICRR* expression levels. Based on the 691 differentially expressed mRNAs between high- and low- *TICRR* expression groups, we analyzed interactions using the STRING database, where the interaction threshold was set as 0.4. The line represents protein-protein interactions. The darker the filling color, the more mRNA interactions.

Supplementary Figure 3 | Mean decrease Gini plot for important indexes associated with overall survival in PRCC patients. The random forest model was used to rank significant indexes, enrolling age, sex, smoking history, serum calcium level, hemoglobin level, TMN stage, clinical stage, and *TICRR* expression.

Supplementary Table 1 | Top 20 clusters in pathway and process enrichment analysis of DEGs in PRCC patients with distinct *TICRR* levels.

REFERENCES

Akhtar, M., Al-Bozom, I. A., and Al Hussain, T. (2019). Papillary renal cell carcinoma (PRCC): an Update. *Adv. Anat. Pathol.* 26, 124–132.doi: 10.1097/pap.0000000000000220

Alshenawy, H. A. (2015). Immunohistochemical panel for differentiating renal cell carcinoma with clear and papillary features. *Pathol. Oncol. Res.* 21, 893–899.doi: 10.1007/s12253-015-9898-7

Beckhove, P., Feuerer, M., Dolenc, M., Schuetz, F., Choi, C., Sommerfeldt, N., et al. (2004). Specifically activated memory T cell subsets from cancer patients recognize and reject xenotransplanted autologous tumors. *J. Clin. Invest.* 114, 67–76.doi: 10.1172/jci20278

Blighe, K. (2019). *EnhancedVolcano: Publication-Ready Volcano Plots With Enhanced Colouring and Labeling*.

Boos, D., Sanchez-Pulido, L., Rappas, M., Pearl, L. H., Oliver, A. W., Ponting, C. P., et al. (2011). Regulation of DNA replication through Sld3-Dpb11 interaction is conserved from yeast to humans. *Curr. Biol.* 21, 1152–1157.doi: 10.1016/j.cub.2011.05.057

Bruck, I., and Kaplan, D. L. (2015). Conserved mechanism for coordinating replication fork helicase assembly with phosphorylation of the helicase. *Proc. Natl. Acad. Sci. U.S.A.* 112, 11223–11228.doi: 10.1073/pnas.1509608112

Bruck, I., Perez-Arnaiz, P., Colbert, M. K., and Kaplan, D. L. (2015). Insights into the initiation of eukaryotic DNA replication. *Nucleus* 6, 449–454.doi: 10.1080/19491034.2015.1115938

Cao, Q., Ruan, H., Wang, K., Song, Z., Bao, L., Xu, T., et al. (2018). Overexpression of PLIN2 is a prognostic marker and attenuates tumor progression in clear cell renal cell carcinoma. *Int. J. Oncol.* 53, 137–147. doi: 10.3892/ijo.2018.4384

Charrasse, S., Gharbi-Ayachi, A., Burgess, A., Vera, J., Hached, K., Raynaud, P., et al. (2017). Ensa controls S-phase length by modulating Treslin levels. *Nat. Commun.* 8:206. doi: 10.1038/s41467-017-00339-4

Donskov, F. (2013). Immunomonitoring and prognostic relevance of neutrophils in clinical trials. *Semin. Cancer Biol.* 23, 200–207.doi: 10.1016/j.semcancer.2013.02.001

Farber, N. J., Kim, C. J., Modi, P. K., Hon, J. D., Sadimin, E. T., and Singer, E. A. (2017). Renal cell carcinoma: the search for a reliable biomarker. *Transl. Cancer Res.* 6, 620–632. doi: 10.21037/tcr.2017.05.19

Fernandes, D. S., and Lopes, J. M. (2015). Pathology, therapy and prognosis of papillary renal carcinoma. *Future Oncol.* 11, 121–132.doi: 10.2217/fon.14.133

Fu, C., and Jiang, A. (2018). Dendritic cells and CD8 T Cell immunity in tumor microenvironment. *Front. Immunol.* 9:3059. doi: 10.3389/fimmu.2018.03059

Hänzelmann, S., Castelo, R., and Guinney, J. (2013). GSVA: gene set variation analysis for microarray and RNA-seq data. *BMC Bioinformatics* 14:7.doi: 10.1186/1471-2105-14-7

Harrell, F. E. Jr. (2020). *rms: Regression Modeling Strategies*.

Kolde, R. (2019). *ptheatmap: Pretty Heatmaps*.

Liu, J., Lichtenberg, T., Hoadley, K. A., Poisson, L. M., Lazar, A. J., Cherniack, A. D., et al. (2018). An integrated TCGA pan-cancer clinical data resource to drive high-quality survival outcome analytics. *Cell* 173, 400.e11–416.e11. doi: 10.1016/j.cell.2018.02.052

Love, M. I., Huber, W., and Anders, S. (2014). Moderated estimation of fold change and dispersion for RNA-seq data with DESeq2. *Genome Biol.* 15:550. doi: 10.1186/s13059-014-0550-8

Max Gordon, T. L. (2020). *forestplot: Advanced Forest Plot Using 'grid' Graphics*.

Maya-Mendoza, A., Moudry, P., Merchut-Maya, J. M., Lee, M., Strauss, R., and Bartek, J. (2018). High speed of fork progression induces DNA replication stress and genomic instability. *Nature* 559, 279–284.doi: 10.1038/s41586-018-0261-5

Merad, M., Sathe, P., Helft, J., Miller, J., and Mortha, A. (2013). The dendritic cell lineage: ontogeny and function of dendritic cells and their subsets in the steady state and the inflamed setting. *Annu. Rev. Immunol.* 31, 563–604.doi: 10.1146/annurev-immunol-020711-074950

Morabito, R. A., Talug, C., Zaslau, S., and Kandzari, S. (2010). Asymptomatic advanced pediatric papillary renal cell carcinoma presenting as a pulmonary embolus. *Urology* 76, 153–155.doi: 10.1016/j.urology.2009.09.016

Peng, D., Zhang, C. J., Tang, Q., Zhang, L., Yang, K. W., Yu, X. T., et al. (2018). Prognostic significance of the combination of preoperative hemoglobin and albumin levels and lymphocyte and platelet counts (HALP) in patients with renal cell carcinoma after nephrectomy. *BMC Urol.* 18:20. doi: 10.1186/s12894-018-0333-8

Qu, X., Tang, Y., and Hua, S. (2018). Immunological approaches towards cancer and inflammation: a cross talk. *Front. Immunol.* 9:563. doi: 10.3389/fimmu.2018.00563

Reading, J. L., Gálvez-Cancino, F., Swanton, C., Lladser, A., Peggs, K. S., and Quezada, S. A. (2018). The function and dysfunction of memory CD8(+) T cells in tumor immunity. *Immunol. Rev.* 283, 194–212.doi: 10.1111/imr.12657

Shannon, P., Markiel, A., Ozier, O., Baliga, N. S., Wang, J. T., Ramage, D., et al. (2003). Cytoscape: a software environment for integrated models of biomolecular interaction networks. *Genome Res.* 13, 2498–2504.doi: 10.1101/gr.1239303

Siegel, R. L., Miller, K. D., and Jemal, A. (2018). Cancer statistics, 2018. *CA Cancer J. Clin.* 68, 7–30.doi: 10.3322/caac.21442

Song, J., Liu, Y. D., Su, J., Yuan, D., Sun, F., and Zhu, J. (2019). Systematic analysis of alternative splicing signature unveils prognostic predictor for kidney renal clear cell carcinoma. *J. Cell. Physiol.* 234, 22753–22764. doi: 10.1002/jcp.28840

Srigley, J. R., Delahunt, B., Eble, J. N., Egevad, L., Epstein, J. I., Grignon, D., et al. (2013). The International Society of Urological Pathology (ISUP) Vancouver Classification of Renal Neoplasia. *Am. J. Surg. Pathol.* 37, 1469–1489.doi: 10.1097/PAS.0b013e318299f2d1

Subramanian, A., Tamayo, P., Mootha, V. K., Mukherjee, S., Ebert, B. L., Gillette, M. A., et al. (2005). Gene set enrichment analysis: a knowledge-based approach for interpreting genome-wide expression profiles. *Proc. Natl. Acad. Sci. U.S.A.* 102, 15545–15550.doi: 10.1073/pnas.0506580102

Svetnik, V., Liaw, A., Tong, C., Culberson, J. C., Sheridan, R. P., and Feuston, B. P. (2003). Random forest: a classification and regression tool for compound classification and QSAR modeling. *J. Chem. Inf. Comput. Sci.* 43, 1947–1958.doi: 10.1021/ci034160g

Szklarczyk, D., Gable, A. L., Lyon, D., Junge, A., Wyder, S., Huerta-Cepas, J., et al. (2019). STRING v11: protein-protein association networks with increased coverage, supporting functional discovery in genome-wide experimental datasets. *Nucleic Acids Res.* 47, D607–D613. doi: 10.1093/nar/gky1131

Xie, L., Wang, Q., Dang, Y., Ge, L., Sun, X., Li, N., et al. (2019a). OSkirc: a web tool for identifying prognostic biomarkers in kidney renal clear cell carcinoma. *Future Oncol.* 15, 3103–3110.doi: 10.2217/fon-2019-0296

Xie, L., Wang, Q., Nan, F., Ge, L., Dang, Y., Sun, X., et al. (2019b). OSacc: gene expression-based survival analysis web tool for adrenocortical carcinoma. *Cancer Manag. Res.* 11, 9145–9152.doi: 10.2147/cmar.S215586

Yan, Z., Wang, Q., Lu, Z., Sun, X., Song, P., Dang, Y., et al. (2020). OSluca: an interactive web server to evaluate prognostic biomarkers for lung cancer. *Front. Genet.* 11:420. doi: 10.3389/fgene.2020.00420

Yan, Z., Wang, Q., Sun, X., Ban, B., Lu, Z., Dang, Y., et al. (2019). OSbrca: a web server for breast cancer prognostic biomarker investigation with massive data from tens of cohorts. *Front. Oncol.* 9:1349. doi: 10.3389/fonc.2019.01349

Yu, G., Wang, L. G., Han, Y., and He, Q. Y. (2012). clusterProfiler: an R package for comparing biological themes among gene clusters. *Omics* 16, 284–287.doi: 10.1089/omi.2011.0118

Yu, Q., Pu, S. Y., Wu, H., Chen, X. Q., Jiang, J. J., Gu, K. S., et al. (2019). TICRR contributes to tumorigenesis through accelerating DNA replication in Cancers. *Front. Oncol.* 9:516. doi: 10.3389/fonc.2019.00516

Zhou, Y., Zhou, B., Pache, L., Chang, M., Khodabakhshi, A. H., Tanaseichuk, O., et al. (2019). Metascape provides a biologist-oriented resource for the analysis of systems-level datasets. *Nat. Commun.* 10:1523. doi: 10.1038/s41467-019-09234-6

Conflict of Interest: The authors declare that the research was conducted in the absence of any commercial or financial relationships that could be construed as a potential conflict of interest.